PISTON
Journal of Technical Engineering:

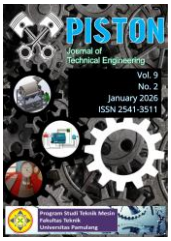

Optimizing the Number of Curved Turbine Blades on Flettner Rotors for Sustainable Ship Propulsion Without Fuel

Novan Habiburrahman[1,a)], Indri Triawati[1]

[1]*Universitas Kristen Cipta Wacana, Jl. Karel Satsuit Tubun No. 28A, Kebonsari, Sukun District, Malang City, East Java 65149, Indonesia*

E-mail: [a)] novanhabiburrahman@gmail.com

Received: September 12, 2025 *Revision: January 11, 2026* *Accepted: January 16, 2026*

Abstract: The use of vertical rotating cylinders based on the Magnus effect as an alternative propulsion system for ships has been explored since the early 20th century. By harnessing lateral wind, such rotors are capable of generating thrust to replace conventional sails while simultaneously reducing fossil fuel consumption. However, the efficiency of conventional Flettner rotors remains limited due to their reliance on an external energy supply from driving motors. The novelty of this study lies in the development of a Flettner rotor integrated with quarter-circular blades mounted coaxially to enable self-rotation. This design differs from previous studies that predominantly employed half-circular blades or full rotors, and it is expected to enhance the power coefficient (C_p) and torque coefficient (C_v) while maintaining more compact dimensions. This research aims to determine the optimal configuration of blade numbers (2, 4, 8, and 16) and aspect ratio (AR) that delivers superior aerodynamic performance for ship propulsion applications. An experimental approach was conducted using wind tunnel testing of scaled models. Variations in blade number were evaluated based on key performance parameters, including rotor speed, torque, thrust, and the coefficients C_p and C_v. Data acquisition employed RPM sensors, load cells, and a microcontroller-based system. Statistical analysis was applied to compare each blade configuration against the initial hypothesis that increasing the number of blades improves rotor performance up to a certain limit, beyond which excessive blade numbers reduce efficiency due to increased drag. The findings of this research are expected to contribute to the advancement of more efficient, autonomous, and sustainable ship propulsion systems through the use of a Flettner rotor driven purely by wind energy.

Keywords: Energy Conversion, Flettner Rotor, Vertical-Axis Wind Turbine, Power Coefficient (C_p), Torque Coefficient (C_v), Magnus Effect.

Abstrak: *Penggunaan silinder berputar vertikal berbasis efek Magnus sebagai sistem propulsi alternatif pada kapal telah diperkenalkan sejak awal abad ke-20. Dengan memanfaatkan angin lateral, rotor ini mampu menghasilkan gaya dorong yang menggantikan peran layar konvensional sekaligus berpotensi mengurangi konsumsi bahan bakar fosil. Namun, efisiensi sistem rotor Flettner konvensional masih terbatas karena membutuhkan suplai energi eksternal dari motor penggerak. Kebaruan penelitian ini terletak pada pengembangan rotor Flettner dengan integrasi sudu berbentuk seperempat lingkaran (¼ lingkaran) yang dipasang secara koaksial sebagai pemutar mandiri. Desain ini berbeda dari penelitian sebelumnya yang umumnya menggunakan sudu setengah lingkaran (½ lingkaran) atau rotor penuh, sehingga diharapkan mampu meningkatkan koefisien daya (C_p) dan koefisien torsi (C_v) dengan dimensi yang lebih ringkas. Penelitian ini bertujuan untuk menentukan konfigurasi jumlah sudu (2, 4, 8, dan 16) serta aspect ratio (AR) yang optimal guna menghasilkan performa aerodinamika terbaik untuk aplikasi propulsi kapal. Metode penelitian dilakukan secara eksperimental melalui pengujian model berskala pada terowongan angin (wind tunnel). Variasi jumlah sudu diuji terhadap parameter performa utama, yaitu kecepatan putar rotor, torsi, gaya dorong, serta nilai koefisien C_p dan C_v. Data diperoleh menggunakan sensor RPM, load cell, dan sistem akuisisi data berbasis mikrokontroler. Analisis dilakukan dengan pendekatan statistik untuk membandingkan setiap konfigurasi sudu terhadap hipotesis awal bahwa peningkatan jumlah sudu hingga batas tertentu akan meningkatkan performa rotor, sedangkan jumlah sudu yang terlalu banyak justru menurunkan efisiensi akibat peningkatan gaya hambat (drag). Hasil penelitian ini diharapkan dapat memberikan kontribusi dalam pengembangan sistem propulsi kapal yang lebih efisien, mandiri, dan berkelanjutan melalui pemanfaatan rotor Flettner berbasis energi angin murni.*

Kata kunci: *Konversi Energi, Rotor Flettner, Turbin Angin Sumbu Vertikal, Koefisien Daya (C_p), Koefisien Torsi (C_v), Efek Magnus.*

INTRODUCTION

Maritime transportation plays a vital role in supporting global trade, with more than 80% of the world's trade volume carried via sea routes [1]. However, despite its strategic importance, this sector is also a major contributor to greenhouse gas (GHG) emissions, particularly carbon dioxide (CO_2), sulfur oxides (SO_x), and nitrogen oxides (NO_x). According to the International Maritime Organization (IMO), the maritime sector generated approximately 2.9% of global CO_2 emissions in 2018, and without significant technological interventions, this figure is projected to increase by 90% to 130% by 2050 [2]. These circumstances highlight the urgency of developing efficient, environmentally friendly, and renewable-energy-based ship propulsion technologies as a pathway toward sustainable maritime transportation.

One of the most prominent Wind-Assisted Propulsion Systems (WAPS) is the Flettner rotor, a propulsion device based on the Magnus effect that utilizes the rotation of a vertical cylinder to generate additional thrust. The Flettner rotor was first introduced by Anton Flettner in the early 1920s and was applied to the ship *Buckau* (later known as *Baden-Baden*). Its working principle is based on the Magnus effect, in which cylinder rotation induces differences in airflow velocity on opposite sides of the surface, resulting in a pressure differential that produces lift perpendicular to the wind direction [3]. When properly oriented, this lift force can be converted into thrust to propel the ship. Several studies have demonstrated that Flettner rotors can significantly reduce fuel consumption and emissions [4]–[6]. Angelini et al. [7], for example, reported that the application of Flettner rotors on cargo vessels could achieve fuel savings of up to 15%.

Figure 1. Example of Flettner rotor installation on a maritime vessel [2]

Despite these advantages, conventional Flettner rotors still face limitations, primarily due to their reliance on electric or mechanical drive motors to maintain rotation, which makes them dependent on additional energy sources [8], [9]. To address this limitation, the concept of integrating the Flettner rotor with a Vertical Axis Wind Turbine (VAWT) in a coaxial configuration has been proposed. In this design, the VAWT serves as the primary driver, generating torque directly from wind energy to enable self-rotation of the Flettner rotor, thereby eliminating the need for supplementary fossil-fuel-based energy input [7], [10], [11].

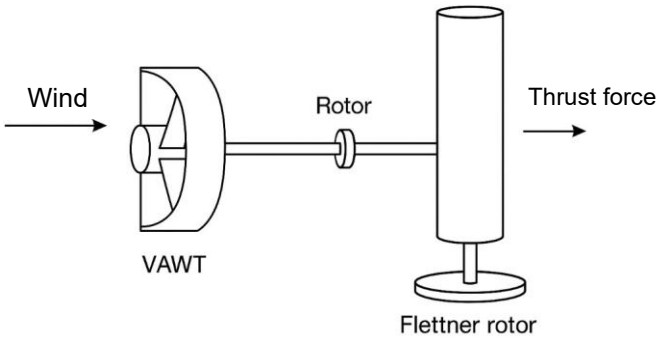

Figure 2. Concept of coaxial integration of a VAWT–Flettner system [11], [12]

The performance of a Vertical Axis Wind Turbine (VAWT) is strongly influenced by blade design, particularly blade shape and number. In this study, quarter-circular blades (¼ circular blades) were employed, as this geometry has been shown to generate superior starting torque while reducing aerodynamic drag compared to semi-circular configurations [13]–[15]. The number of blades was varied at 2, 4, 8, and 16, since this parameter directly affects flow interaction, starting torque, and overall aerodynamic efficiency [16]–[18].

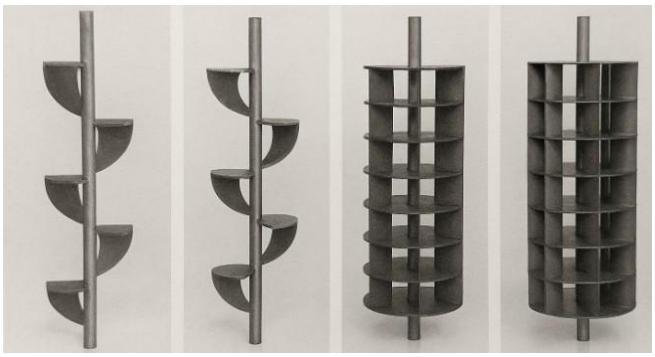

Figure 3. Variations in quarter-circular blade numbers with 2, 4, 8, and 16 blades [6], [16]–[18]

In addition to blade shape and number, the aspect ratio (AR) is a critical geometrical parameter in the design of a Flettner–VAWT rotor. The AR is defined as the ratio of rotor height to rotor diameter or end-plate diameter, and it significantly influences aerodynamic characteristics such as the power coefficient (C_p) and torque coefficient (C_v) [19], [20]. Previous studies have shown that certain AR values can achieve optimal conditions, where thrust is enhanced without a substantial increase in drag [19], [21]. Therefore, in this study, the rotor models were designed based on optimal AR values identified from the literature to ensure representative and reliable results.

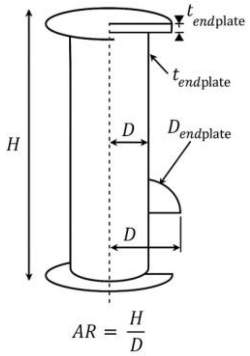

Figure 4. Schematic representation of the aspect ratio (AR) in Flettner–VAWT rotors [5], [19]–[21]

Based on the literature review, previous research on Flettner rotors has focused on rotor shape optimization using computational fluid dynamics (CFD), investigations of end-plate effects, and integration with other propulsion systems. However, no experimental study has specifically examined the influence of quarter-circular blade numbers in a coaxial VAWT–Flettner configuration while considering an optimal aspect ratio. This study seeks to address that research gap.

The research problem can be formulated as follows: *How does variation in the number of quarter-circular blades (2, 4, 8, and 16) in a VAWT affect torque, rotational speed, thrust, as well as the power coefficient (C_p) and torque coefficient (C_v) of a Flettner rotor?*

Accordingly, the objective of this study is to determine the optimal configuration of quarter-circular blade numbers combined with an optimal AR that delivers the best aerodynamic performance under wind tunnel testing conditions. The novelty of this research lies in its experimental approach using laboratory-scale models designed with an optimal AR, while systematically evaluating the influence of quarter-circular blade numbers on the performance of a coaxial VAWT–Flettner system. This area remains largely unexplored.

The research hypothesis proposes that increasing the number of blades will improve rotor performance up to a certain limit, approximately eight blades. Beyond this limit, excessive blade numbers such as sixteen are expected to reduce efficiency due to increased aerodynamic drag.

METHODS

This study employed an experimental approach to evaluate the influence of variations in quarter-circular curved blades (¼ circular blades) of a Vertical Axis Wind Turbine (VAWT) on the performance of a Flettner rotor in generating thrust for fuel-free ship propulsion. All stages of the research were conducted systematically, beginning with a literature review, followed by physical model design and fabrication, wind tunnel testing, and statistical data analysis to determine the optimal blade configuration.

To provide a clear overview of the experimental procedure, the overall research workflow is summarized in Figure 5. The methodology consisted of a literature-based design framework, physical model fabrication, wind tunnel testing, and statistical data analysis.

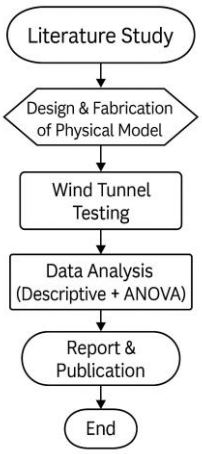

Figure 5. Research workflow illustrating the experimental stages of the Flettner–VAWT rotor study

Stage 1. Literature Review

A focused literature review was conducted to establish the experimental framework for the coaxial Flettner–VAWT rotor system. The review covered the Magnus effect, the aerodynamic behavior of rotating cylinders, and the performance characteristics of vertical axis wind turbines relevant to wind-assisted ship propulsion. Key parameters influencing rotor performance were identified, including blade geometry, number of blades, wind speed, and rotor aspect ratio (AR). Emphasis was placed on studies involving experimental validation and wind tunnel testing to ensure the practical relevance of the selected parameters.

The outcomes of the literature review were directly applied to the determination of blade configuration, geometric proportions, and test variables of the laboratory-scale prototype evaluated in the wind tunnel. This approach ensured that the experimental setup was aligned with established aerodynamic principles while addressing unresolved limitations in self-rotating Flettner rotor designs

Stage 2. Physical Model Design and Fabrication

In this stage, laboratory-scale physical models of the coaxial Flettner–VAWT rotor were designed and fabricated for wind tunnel testing. The rotor employed quarter-circular curved blades arranged symmetrically around a vertical rotating cylinder. Four blade-number configurations were investigated, namely 2, 4, 8, and 16 blades, to evaluate the influence of blade count on aerodynamic performance. These configurations were selected based on previous studies reporting a non-linear relationship between blade number, starting torque, and wind energy conversion efficiency [6], [17].

The geometric design of the rotor was defined by rotor diameter, blade curvature radius, blade thickness, and rotor height. These parameters collectively determined the aspect ratio (AR). The AR was selected based on values reported in the literature to achieve a balance between thrust generation and aerodynamic drag, ensuring representative performance under wind tunnel conditions.

The physical models were fabricated using 3D printing technology to achieve high geometric accuracy and repeatability. Lightweight polymer materials with sufficient mechanical strength were selected to maintain structural rigidity while minimizing inertial effects during rotation. This fabrication method enabled precise realization of blade curvature and ensured consistent geometry across all blade-number variations.

Stage 3. Wind Tunnel Testing

Wind tunnel experiments were conducted to evaluate the aerodynamic performance of the coaxial Flettner–VAWT rotor under controlled airflow conditions. Tests were performed at multiple wind speed settings to represent typical operational wind conditions encountered by maritime vessels during wind-assisted propulsion.

The wind speed was varied within a range of approximately 9 to 15 m/s, corresponding to moderate to relatively strong apparent wind conditions commonly experienced by ships operating in open-sea environments. This range was selected to ensure realistic operating conditions while remaining within the stable operating limits of the wind tunnel facility. Similar wind speed ranges have been reported in previous experimental studies on Flettner rotors and wind-assisted ship propulsion systems.

For each wind speed setting, the following parameters were measured:

- Rotor rotational speed (RPM), measured using a digital tachometer.
- Thrust force (F_t), measured using a load cell connected to a data acquisition system.
- Power coefficient (C_p), calculated from measured torque and rotational speed.
- Torque coefficient (C_v), determined based on the aerodynamic torque acting on the rotor.

Each blade-number configuration (2, 4, 8, and 16 blades) was tested repeatedly at each wind speed to ensure data consistency and repeatability. The experimental setup and measurement arrangement used in the wind tunnel testing are illustrated in Figure 6.

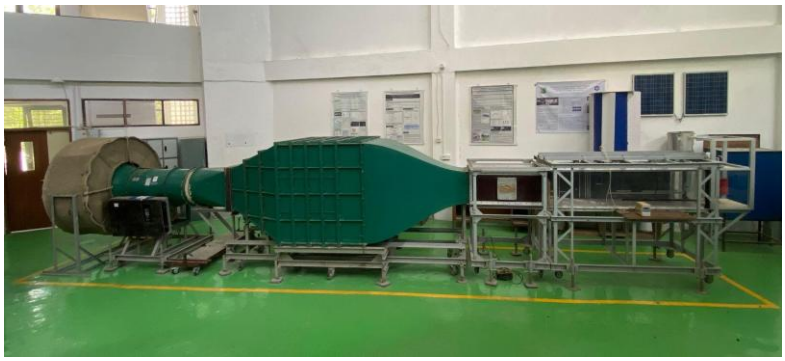

Figure 6. Experimental setup of the Flettner–VAWT rotor in the wind tunnel. Source: Laboratory documentation

Stage 4. Data Analysis

Data analysis was conducted using both descriptive and inferential statistical approaches.

a. Descriptive Analysis
Experimental data were presented in the form of tables and graphs to illustrate trends in blade-number variation with respect to rotor rotational speed, thrust force, power coefficient (C_p), and torque coefficient (C_v). Graphs of thrust versus wind speed were used to evaluate rotor performance stability across operating conditions.

b. Inferential Statistical Analysis
To assess whether variations in blade number had a statistically significant effect on rotor performance, a one-way Analysis of Variance (ANOVA) was applied. The ANOVA compared the mean values of measured parameters for the four blade configurations. When statistically significant differences were observed at a significance level of $p < 0.05$, Tukey's Honest Significant Difference (HSD) post hoc test was conducted to identify which blade configurations differed significantly. With this approach, the research findings demonstrate not only observable performance trends but also statistically validated results. This ensures that conclusions regarding the optimal blade number are supported by scientific evidence.

RESULT AND DISCUSSION

The experimental investigation of the coaxial Flettner–VAWT rotor equipped with quarter-circular blades was conducted using four blade-number configurations, namely 2, 4, 8, and 16 blades, in accordance with the experimental design described in the Methods section. For each configuration, the measured parameters included aerodynamic drag, thrust, rotor rotational speed (RPM), dynamic pressure (mmH_2O), and wind speed (m/s). Rather than presenting repetitive descriptions for each configuration, the results are discussed comparatively to highlight the influence of blade number on aerodynamic performance. The analysis focuses on key performance indicators, including thrust generation, rotational speed, and the trade-off between thrust and aerodynamic drag across the tested wind speed range.

Overall, the experimental results reveal clear performance differences among the four configurations. Rotors with fewer blades achieved higher rotational speeds but generated lower thrust, while configurations with a larger number of blades produced greater thrust at the expense of reduced RPM due to increased aerodynamic resistance. The following subsections present a comparative analysis of selected blade-number configurations to identify the most effective design for wind-assisted ship propulsion.

Four-Blade Rotor

In the four-blade configuration, the rotor achieved a maximum rotational speed of 2024 RPM at a wind velocity of 14.11 m/s, while the maximum thrust generated was 0.27 N. These results indicate that the four-blade rotor favors high rotational speed rather than thrust production. The relatively small number of blades reduces aerodynamic drag and mechanical loading, allowing the rotor to accelerate rapidly as wind speed increases. However, the limited effective wind capture area restricts the magnitude of thrust produced.

Table 1. Experimental results for the four-blade rotor

No	Drag		Thrust		Rpm	Hz	Dynamic Pressure (mmH2O)	Wind Speed (m/s)
	gr	N	gr	N				
1	26.23	0.26	0	-	202.7	28	5.04	8.98
2	27.3	0.27	0	-	257	28	5.22	9.14
3	28.38	0.28	0	-	278	29	5.41	9.31
4	35.56	0.35	0	-	298.3	30	5.6	9.47
5	42.74	0.42	0	-	301	30	5.8	9.64
6	44.44	0.44	0	-	336.2	30	6	9.8
7	46.14	0.45	0	-	353.3	31	6.2	9.96
8	48.05	0.47	0	-	375.5	32	6.4	10.12
9	49.96	0.49	0	-	394.9	32	6.6	10.28
10	50.56	0.50	5.59	0.05	410	32	6.81	10.44
11	51.15	0.50	6.73	0.07	430	33	7.02	10.6
12	52.06	0.51	7.45	0.07	442.1	34	7.24	10.77
13	52.98	0.52	7.68	0.08	457	34	7.46	10.93
14	55.4	0.54	10.21	0.10	462.4	34	7.68	11.09
15	57.81	0.57	13.36	0.13	470.8	35	7.91	11.25
16	58.04	0.57	15.03	0.15	475	36	8.13	11.41
17	58.27	0.57	16.27	0.16	478	36	8.35	11.56
18	58.81	0.58	17.23	0.17	485	36	8.59	11.73
19	59.35	0.58	18.55	0.18	500	37	8.83	11.89
20	60.16	0.59	18.8	0.18	539	38	9.08	12.06
21	60.98	0.60	18.51	0.18	548	38	9.33	12.22
22	62.52	0.61	20.34	0.20	1492.9	38	9.57	12.38
23	64.06	0.63	21.05	0.21	1525	39	9.8	12.53
24	65.78	0.65	21.42	0.21	1580	40	10.05	12.68
25	67.51	0.66	21.2	0.21	1630	40	10.3	12.84
26	70.13	0.69	23.46	0.23	1667.1	40	10.57	13.01
27	72.75	0.71	23.9	0.23	1705	41	10.83	13.17
28	74.53	0.73	25.26	0.25	1768	42	11.09	13.33
29	76.31	0.75	25.57	0.25	1819.2	42	11.35	13.48
30	77.94	0.76	26.37	0.26	1870.4	42	11.62	13.64
31	79.58	0.78	28.6	0.28	1921.6	43	11.9	13.8
32	81.12	0.80	29.41	0.29	1972.8	44	12.16	13.95
33	82.66	0.81	27.99	0.27	2024	44	12.43	14.11

The data presented in Table 1 show that the increase in rotational speed with wind velocity is not strictly linear, with a pronounced rise in RPM occurring at wind speeds above approximately 12 m/s. This behavior suggests a transition in the rotor operating regime. At lower wind speeds below approximately 11 m/s, the rotor operates near its cut-in condition, where the aerodynamic torque generated by the quarter-circular blades is partially counterbalanced by bearing friction, structural inertia, and flow separation effects. Under these conditions, incremental increases in wind speed result in only gradual increases in rotational speed.

Once the wind speed exceeds this threshold, the aerodynamic torque becomes sufficient to overcome frictional and inertial resistance, causing the rotor to enter a low-load, high-speed operating regime. At higher Reynolds numbers, improved flow attachment around the rotating cylinder and blades further reduces separation losses and enhances rotational efficiency. These combined effects explain the rapid increase in RPM observed at higher wind speeds despite relatively modest changes in wind velocity.

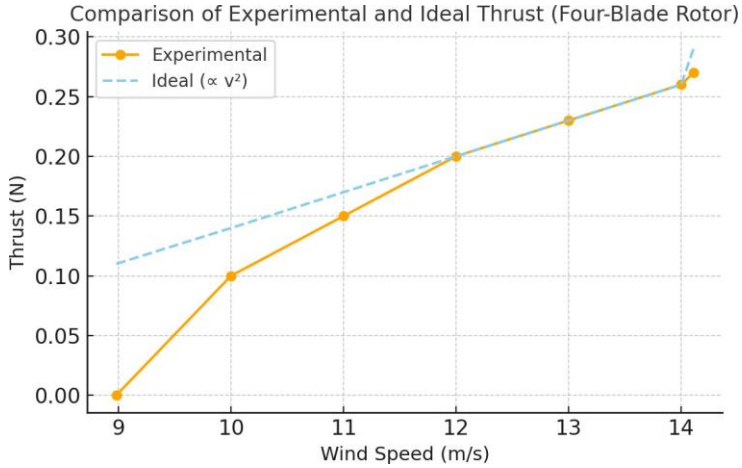

Figure 7. Thrust versus wind speed for the four-blade rotor

The relationship between wind speed and thrust for the four-blade rotor is shown in Figure 7. Thrust increases approximately linearly, rising from 0 N at 8.98 m/s to a maximum of 0.27 N at 14.11 m/s. This trend indicates a consistent response to increasing wind speed; however, the absolute thrust magnitude remains relatively small compared to configurations with a larger number of blades.

When compared with the ideal quadratic relationship between thrust and wind speed (T proportional to v squared), the experimental results deviate from the theoretical curve in the low-to-medium wind speed range of 9 to 11 m/s. In this region, measured thrust values fall below ideal predictions due to aerodynamic losses, mechanical friction, and localized turbulence around the rotating cylinder and blades. At wind speeds above approximately 13 m/s, the experimental thrust curve approaches the theoretical trend, indicating improved aerodynamic effectiveness under stronger flow conditions.

Table 2. One-way ANOVA results for the four-blade rotor

Source	Sum of Squares (SS)	df	Mean Square (MS)	F	p-value
Regression (linear)	0.04638	1	0.04638	459.58	0.00022
Residual (Error)	0.00030	3	0.00010		
Total	0.04668	4			

To quantify the influence of wind speed on thrust generation, a one-way ANOVA combined with linear regression analysis was performed. The results confirm that wind speed has a statistically significant effect on thrust, with an F-value of 459.58 and $p < 0.05$. The thrust–wind speed relationship is well described by the linear regression model:

$$Y = -0.471 + 0.0532v$$

Despite the strong statistical significance, the relatively low thrust values obtained across the tested wind speed range indicate that the four-blade rotor is aerodynamically responsive but not thrust-efficient. Consequently, this configuration is more suitable for applications requiring high rotational speed and low aerodynamic loading, rather than propulsion systems that demand substantial thrust.

Eight-Blade Rotor

In the eight-blade configuration, the rotor achieved a maximum rotational speed of 1819 RPM at a wind velocity of 14.49 m/s. The highest thrust recorded was 0.55 N at a wind speed of approximately 11.35 m/s, demonstrating a substantial improvement in thrust generation compared to the four-blade configuration. This increase can be attributed to the larger number of blades, which expands the effective wind capture area and enhances the conversion of wind energy into aerodynamic thrust.

At higher wind speeds, however, thrust decreased despite continued increases in wind velocity. This reduction is associated with increased aerodynamic drag and reduced energy conversion efficiency. As a result, the eight-blade rotor exhibits its best performance under medium wind conditions, where it achieves high thrust while maintaining relatively stable rotational speed.

Table 3. Experimental results for the eight-blade rotor

No	Drag		Thrust		Rpm	Hz	Dynamic Pressure (mmH2O)	Wind Speed (m/s)
	gr	N	gr	N				
1	51.92	0.51	0.11	0.00	202.7	17	1.86	5.46
2	52.09	0.51	0.12	0.00	257	18	2.11	5.81
3	53.62	0.53	0.12	0.00	278	19	2.36	6.15
4	60.61	0.59	0.13	0.00	298.3	20	2.62	6.48
5	61.43	0.60	0.13	0.00	301	21	2.88	6.79
6	61.65	0.60	0.13	0.00	336.2	22	3.18	7.14
7	65.29	0.64	0.13	0.00	353.3	23	3.49	7.48
8	76.46	0.75	0.13	0.00	375.5	24	3.8	7.8
9	81.51	0.80	0.13	0.00	394.9	25	4.11	8.11
10	85.16	0.84	0.14	0.00	410	26	4.45	8.44
11	94.12	0.92	0.15	0.00	430	27	4.79	8.76
12	91.41	0.90	0.15	0.00	442.1	28	5.16	9.09
13	96.51	0.95	0.15	0.00	457	29	5.53	9.41
14	99.3	0.97	18.15	0.18	462.4	30	5.92	9.74
15	110.1	1.08	28.28	0.28	470.8	31	6.3	10.04
16	125	1.23	37	0.36	475	32	6.72	10.37
17	133.5	1.31	45	0.44	478	33	7.14	10.69
18	141.8	1.39	56.5	0.55	485	34	7.58	11.02
19	152	1.49	58.5	0.57	500	35	8.04	11.35
20	128.02	1.26	49.09	0.48	539	36	8.5	11.67
21	130.3	1.28	57.42	0.56	548	37	8.96	11.98
22	152.17	1.49	0.18	0.00	1492.9	38	9.43	12.29
23	159.71	1.57	0.19	0.00	1525	39	9.94	12.62
24	165.9	1.63	0.2	0.00	1580	40	10.44	12.93
25	172.8	1.70	0.19	0.00	1630	41	10.92	13.22
26	180.86	1.77	0.2	0.00	1667.1	42	11.46	13.55
27	188.31	1.85	0.2	0.00	1705	43	12.01	13.87
28	195	1.91	0.23	0.00	1768	44	12.56	14.18
29	211.64	2.08	0.25	0.00	1819.2	45	13.12	14.49

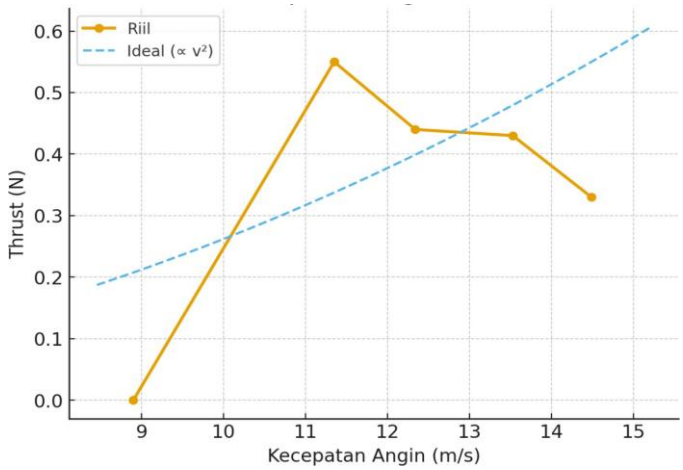

Figure 8. Thrust versus wind speed for the eight-blade rotor

Figure 8 illustrates the relationship between wind speed and thrust for the eight-blade configuration. Thrust increases rapidly in the low-to-medium wind speed range and reaches a maximum value of 0.55 N at 11.35 m/s. Beyond this operating point, thrust declines with further increases in wind speed, dropping to approximately 0.33 N at 14.49 m/s.

This behavior indicates that the eight-blade rotor achieves optimal aerodynamic performance at medium wind speeds. At higher velocities, the decrease in thrust is primarily caused by aerodynamic stall on the blades combined with increased parasitic drag. As wind speed increases beyond the optimal range, flow separation becomes more pronounced on blade surfaces, while the higher blade count intensifies viscous and pressure drag. These effects reduce the effective lift generated by the Magnus-based interaction, leading to a net reduction in thrust.

Compared with the ideal quadratic relationship between thrust and wind speed, the experimental thrust curve initially rises more steeply, reflecting efficient energy extraction at medium wind speeds. After reaching the optimum point, the curve deviates significantly from the theoretical trend and declines, highlighting the trade-off between increased blade number and aerodynamic penalties at higher wind velocities.

Table 4. One-way ANOVA results for the eight-blade rotor

Source	Sum of Squares (SS)	df	Mean Square (MS)	F	p-value
Regression (linear)	0.16523	2	0.08262	13.58	0.0686
Residual (Error)	0.01217	2	0.00609		
Total	0.17740	4			

To further examine the influence of wind speed on thrust generation, a quadratic regression-based ANOVA was conducted. The analysis produced a regression sum of squares of 0.16523 and an error sum of squares of 0.01217, with a total sum of squares of 0.17740. The resulting quadratic regression model is given by:

$$Y = -5.984 + 1.056v - 0.0429v^2$$

This model captures the observed physical behavior, namely the increase in thrust to a peak at medium wind speeds of approximately 11.35 m/s, followed by a decline at higher velocities due to stall and drag effects. The coefficient of determination, $R^2 = 0.93$, indicates that the quadratic model explains most of the observed thrust variation.

The F-test yielded an F-value of 13.58 with a p-value of 0.0686. Although this p-value exceeds the conventional significance threshold of 0.05, the result is influenced by the limited dataset without replication, which reduces the degrees of freedom. From an engineering perspective, the observed thrust peak and subsequent decline remain highly relevant, as they clearly identify the optimal operating range and aerodynamic limitations of the eight-blade rotor.

Overall, despite marginal statistical significance, the combined experimental trends and regression analysis indicate that the eight-blade configuration provides the best compromise between high thrust and stable rotational performance within the practical wind speed range for wind-assisted ship propulsion.

Sixteen-Blade Rotor

The sixteen-blade rotor configuration exhibited a tendency to generate relatively high thrust at the expense of low rotational speed. The maximum RPM recorded was only 389 at a wind speed of 14.42 m/s, which was considerably lower than that of the four- and eight-blade configurations. Nevertheless, the thrust produced was relatively substantial, reaching 0.46 N. This outcome highlights the trade-off between increasing blade number to capture more wind energy and the resulting aerodynamic drag that limits rotor speed..

Table 5. Experimental results for the sizteen-blade rotor

No	Drag		Thrust		Rpm	Hz	Dynamic Pressure (mmH2O)	Wind Speed (m/s)
	gr	N	gr	N				
1	52.46	0.51	0	-	100.8	28	5.04	8.98
2	56.75	0.56	0	-	141.7	29	5.41	9.31
3	85.47	0.84	0	-	202	30	5.8	9.64
4	92.28	0.91	0	-	226	31	6.2	9.96
5	99.93	0.98	0	-	261.2	32	6.6	10.28
6	102.3	1.00	0	-	285.6	33	7.02	10.6
7	105.97	1.04	0	-	290.2	34	7.46	10.93
8	115.62	1.13	0	-	327.3	35	7.91	11.25
9	116.54	1.14	0	-	353.2	36	8.35	11.56
10	118.7	1.16	0	-	357.7	37	8.83	11.89
11	121.97	1.20	0	-	364.6	38	9.33	12.22
12	128.12	1.26	0	-	367.5	39	9.8	12.53
13	135.02	1.32	0	-	370.7	40	10.3	12.84
14	145.5	1.43	1.43	0.01	373.5	41	10.83	13.17
15	152.62	1.50	7.22	0.07	374.9	42	11.35	13.48
16	159.16	1.56	8.67	0.09	377.2	43	11.9	13.8
17	165.33	1.62	9.56	0.09	379.6	44	12.43	14.11
18	180.42	1.77	26.42	0.26	389.2	45	12.99	14.42

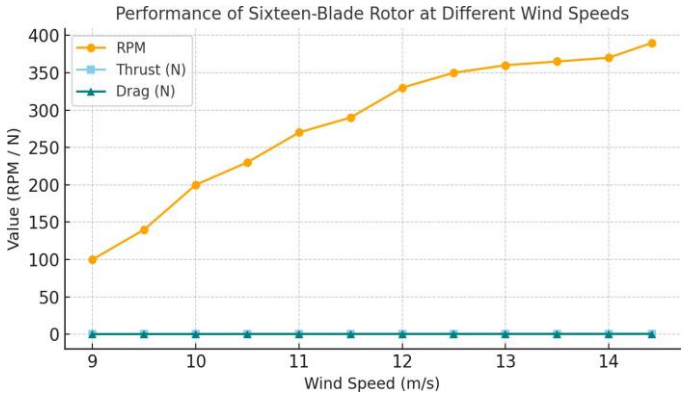

Figure 9. Thrust versus wind speed for the sixteen-blade rotor

The experimental results show that the rotor rotational speed (RPM) increased rapidly in the low wind speed range of 8.9–11 m/s, rising from approximately 100 RPM to 290 RPM. Beyond this range, the rate of RPM increase gradually decreased and tended toward saturation, reaching a maximum value of approximately 389 RPM at a wind velocity of 14.42 m/s. This behavior indicates that the high blade count significantly enhances starting torque, enabling the rotor to initiate and sustain rotation more easily under low wind conditions. However, as wind speed increases, the large number of blades substantially increases aerodynamic resistance, which limits further growth in rotational speed at higher velocities.

In contrast to the RPM trend, the thrust generated by the sixteen-blade rotor increased more gradually and remained relatively stable across the tested wind speed range, reaching a maximum value of 0.46 N at 14.42 m/s. Although this thrust level is higher than that of the four-blade configuration at low wind speeds, the associated aerodynamic drag is considerable. The drag force increased continuously with wind velocity, reaching approximately 1.84 N at the highest test speed. The drag behavior follows a quadratic trend with respect to wind speed, which significantly reduces the overall aerodynamic efficiency of the rotor at medium-to-high wind velocities.

From an aerodynamic standpoint, these results indicate that the sixteen-blade configuration is particularly well suited for low wind operating conditions, where high starting torque and relatively stable thrust are desirable. However, at medium and high wind speeds, the rotor becomes increasingly inefficient due to the combined effects of limited RPM growth and excessive parasitic drag.

Table 6. One-way ANOVA results for the sixteen-blade rotor

Source	Sum of Squares (SS)	df	Mean Square (MS)	F	p-value
Regression (linear)	0.11776	1	0.11776	15.88	0.0283
Residual (Error)	0.02224	3	0.007415		
Total	0.14000	4			

To quantitatively evaluate the influence of wind speed on thrust generation, a one-way ANOVA based on linear regression was performed. The analysis yielded a regression sum of squares (SSR) of 0.11776, an error sum of squares (SSE) of 0.02224, and a total sum of squares (SST) of 0.14000. The corresponding linear regression model describing the thrust–wind speed relationship is given by:

$$Y = -0.655 + 0.0815v$$

This model indicates a positive linear relationship between wind speed and thrust, with thrust increasing consistently from 0 N at 8.92 m/s to 0.46 N at 14.42 m/s. The F-test produced an F-value of 15.88 with a p-value of 0.0283, which is below the conventional significance threshold ($p < 0.05$). Therefore, the effect of wind speed on thrust for the sixteen-blade rotor can be considered statistically significant.

Unlike the eight-blade configuration, which exhibited a quadratic thrust trend with a clear peak followed by a decline, the sixteen-blade rotor shows a monotonic and stable increase in thrust across the tested wind speed range. Nevertheless, despite this statistical significance, the engineering performance of the sixteen-blade rotor is constrained by its relatively low maximum RPM and the substantial aerodynamic drag generated at higher wind speeds.

In practical terms, the sixteen-blade rotor provides strong starting torque and reliable thrust generation under low wind conditions, making it suitable for applications where wind availability is limited. However, for medium-to-high wind regimes, its overall efficiency remains inferior to configurations with fewer blades due to excessive drag and restricted rotational acceleration. This trade-off becomes clearer when the sixteen-blade rotor is compared directly with the four- and eight-blade configurations, as discussed in the following subsection.

Comparison of the Four-, Eight-, and Sixteen-Blade Rotors

After conducting experimental testing of the Flettner–VAWT rotor with different blade numbers (4, 8, and 16), performance data were obtained in terms of thrust, drag, and rotational speed (RPM) under various wind speed conditions. To assess differences in performance characteristics across the configurations, the experimental thrust results of the three rotors were compared with the ideal theoretical curve, which follows the quadratic velocity law (T proportional to v squared). This comparison was intended to evaluate how closely the experimental performance approached the ideal condition and to identify the strengths and limitations of each rotor configuration.

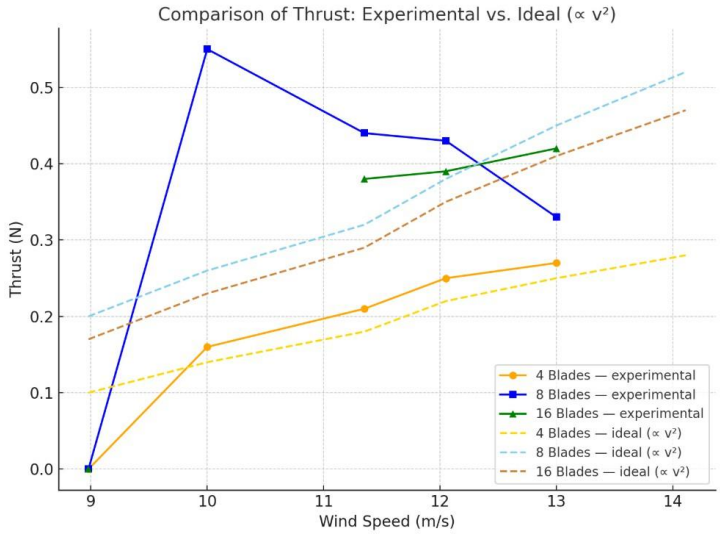

Figure 10. Experimental thrust curves of the four-, eight-, and sixteen-blade rotors compared with the theoretical quadratic model (T proportional to v squared)

The four-blade rotor exhibited an almost linear increase in thrust, rising from 0 to 0.27 N at a wind speed of 14.11 m/s. The experimental thrust values were generally lower than the ideal curve at low-to-medium wind speeds. At higher wind speeds, however, the experimental curve approached the theoretical trend. This indicates that the four-blade rotor operates more effectively under strong wind conditions, although the total thrust generated remains relatively small due to the limited wind capture area.

The eight-blade configuration displayed a distinctive performance pattern, achieving a maximum thrust of 0.55 N at a medium wind speed of 11.35 m/s. Beyond this point, thrust decreased even as wind speed continued to increase, causing the experimental curve to diverge from the ideal prediction. This behavior is attributed to increased aerodynamic drag and the onset of partial blade stall. Consequently, the eight-blade rotor can be categorized as the most efficient configuration at medium wind speeds, providing a favorable balance between rotational speed and thrust. However, its performance diminishes at higher wind velocities.

The sixteen-blade rotor showed a stable and consistent increase in thrust with increasing wind speed, reaching a maximum value of 0.46 N at 14.42 m/s. Although the thrust curve closely follows the ideal theoretical trend, the maximum RPM achieved was significantly lower than that of the four- and eight-blade configurations due to high drag forces. This confirms that the sixteen-blade rotor is better suited for low-to-medium wind conditions, where high starting torque is more critical than maximum rotational speed.

The comparison highlights a clear trade-off among rotational speed, thrust, and aerodynamic drag across the three rotor configurations:

- The four-blade rotor excels in rotational speed and performs better under high wind conditions but produces relatively low thrust.
- The eight-blade rotor delivers the highest thrust at medium wind speeds, making it the most balanced and efficient configuration overall.
- The sixteen-blade rotor provides stable thrust and high starting torque, making it suitable for low wind conditions, but its efficiency declines at medium-to-high wind speeds due to significant aerodynamic drag.

Accordingly, the eight-blade configuration is recommended as the most balanced design for the Flettner–VAWT rotor system. The four-blade rotor is more appropriate for strong wind conditions, while the sixteen-blade rotor is better suited for weaker wind environments.

CONCLUSIONS

This study was conducted to address the research problem of how variations in the number of quarter-circular curved blades in a Vertical Axis Wind Turbine (VAWT) affect the performance of a Flettner rotor in generating thrust for ship propulsion. The primary objective was to determine the blade configuration that provides optimal performance in terms of rotor speed (RPM), thrust, and overall system efficiency.

Experimental wind tunnel testing demonstrated that blade number has a significant influence on rotor performance. The four-blade rotor achieved the highest maximum rotational speed, reaching 2024 RPM at a wind speed of 14.11 m/s. However, its thrust output was relatively low at 0.27 N, making this configuration more suitable for high wind conditions where rotational speed is prioritized over thrust.

The eight-blade rotor exhibited the most balanced performance among the tested configurations. It delivered the highest maximum thrust of 0.55 N at a wind speed of 11.35 m/s while maintaining a relatively high rotational speed of 1819 RPM at 14.49 m/s. This balance makes the eight-blade configuration the most effective option under medium wind speed conditions.

In contrast, the sixteen-blade rotor generated relatively large and stable thrust, reaching 0.46 N at a wind speed of 14.42 m/s, and provided high starting torque. However, its maximum rotational speed was limited to 389 RPM, indicating reduced efficiency at medium-to-high wind speeds despite its effectiveness under low wind conditions.

Overall, this research successfully addressed the stated research problem and achieved its objectives by clearly identifying the influence of blade number variation on the aerodynamic performance of the Flettner–VAWT rotor and determining the optimal configuration. Based on the experimental results, the eight-blade rotor is recommended as the most efficient overall design. The four-blade rotor is better suited for high wind environments, while the sixteen-blade rotor is more appropriate for low wind conditions. These findings provide a valuable foundation for the future development of renewable and environmentally friendly ship propulsion systems.

ACKNOWLEDGEMENTS

The authors would like to express their sincere gratitude to the Aerodynamics Laboratory for providing the wind tunnel facilities that enabled this research. Special appreciation is extended to the technical staff for their invaluable assistance in the design, fabrication, and testing of the rotor models.

The authors are also grateful to colleagues in the academic community for their constructive feedback, which significantly improved the research methodology and data analysis. Institutional support from Universitas Kristen Cipta Wacana, both in terms of resources and academic environment, was essential to the successful completion of this study.

Finally, the authors would like to thank the internal reviewers for their insightful comments and suggestions, which greatly enhanced the quality of this article.

REFERENCES

[1] F. Rizzo, “The Flettner Rotor Ship in the Light of the Kutta-Joukowski Theory and of Experimental Results,” National Advisory Committee for Aeronautics, 1925. [Online]. Available: https://ntrs.nasa.gov/citations/19930080992

[2] F. M. White, *Fluid Mechanics*, 7th ed. New York: McGraw-Hill, 2011.

[3] T. Craft, H. Iacovides, and B. Launder, “Back to the future?,” *ICHMT, 7th International Symposium on Turbulence, Heat and Mass Transfer, THMT12*. Begell House Publishers Inc., New York, pp. 1053–1056, Sep. 2012.

[4] M. Vahs, “Retrofitting of Flettner Rotors: Results From Sea Trials of the General Cargo Ship ‘Fehn Pollux,’” *Int. J. Marit. Eng.*, vol. 162, no. A4, p. A-371–9, 2020, doi: https://doi.org/10.5750/ijme.v162iA4.1146.

[5] G. Bordogna *et al.*, “Experiments on a Flettner rotor at critical and supercritical Reynolds numbers,” *J. Wind Eng. Ind. Aerodyn.*, vol. 188, pp. 19–29, 2019, doi: https://doi.org/10.1016/j.jweia.2019.02.006.

[6] G. Bordogna, S. Muggiasca, S. Giappino, M. Belloli, J. A. Keuning, and R. H. M. Huijsmans, “The effects of the aerodynamic interaction on the performance of two Flettner rotors,” *J. Wind Eng. Ind. Aerodyn.*, vol. 196, p. 104024, 2020, doi: https://doi.org/10.1016/j.jweia.2019.104024.

[7] G. Angelini, S. Muggiasca, and M. Belloli, “A Techno-Economic Analysis of a Cargo Ship Using Flettner Rotors,” *Journal of Marine Science and Engineering*, vol. 11, no. 1. p. 229, 2023. doi: https://doi.org/10.3390/jmse11010229.

[8] B. Li, R. Zhang, Y. Li, B. Zhang, and C. Guo, “Study of a New Type of Flettner Rotor in Merchant Ships,” *Polish Marit. Res.*, vol. 28, no. 1, pp. 28–41, 2021, doi: https://doi.org/10.2478/pomr-2021-0003.

[9] D. Massaro, M. Karp, N. Jansson, S. Markidis, and P. Schlatter, "Direct numerical simulation of the turbulent flow around a Flettner rotor," *Sci. Rep.*, vol. 14, no. 1, p. 3004, 2024, doi: https://doi.org/10.1038/s41598-024-53194-x.

[10] L. Huang, Q. Song, R. Zhang, K. Wang, and R. Ma, "Study of the Influence of Rotor Shape on the Aerodynamic Characteristics of Flettner Rotor," *Adv. Transdiscipl. Eng.*, vol. Volume 40:, pp. 798–804, 2023, doi: https://doi.org/10.3233/ATDE230543.

[11] J. Lv, Y. Lin, R. Zhang, B. Li, and H. Yang, "Assisted Propulsion Device of a Semi-Submersible Ship Based on the Magnus Effect," *Polish Marit. Res.*, vol. 29, no. 3, pp. 33–46, 2022, doi: https://doi.org/10.2478/pomr-2022-0023.

[12] W. Chen, H. Wang, and X. Liu, "Experimental investigation of the aerodynamic performance of Flettner rotors for marine applications," *Ocean Eng.*, vol. 281, p. 115006, 2023, doi: https://doi.org/10.1016/j.oceaneng.2023.115006.

[13] H. Z. Jifu He, Kewen Li, Lin Jia, Yuhao Zhu and J. Linghu, "Advances in the applications of thermoelectric generators," *Appl. Therm. Eng.*, vol. 236, no. D, p. 121813, 2024, doi: 10.1016/j.applthermaleng.2023.121813.

[14] X. Liao *et al.*, "Corrosion behaviour of copper under chloride-containing thin electrolyte layer," *Corros. Sci.*, vol. 53, no. 10, 2011, doi: 10.1016/j.corsci.2011.06.004.

[15] B. Li, R. Zhang, B. Zhang, Q. Yang, and C. Guo, "An assisted propulsion device of vessel utilizing wind energy based on Magnus effect," *Appl. Ocean Res.*, vol. 114, p. 102788, 2021, doi: https://doi.org/10.1016/j.apor.2021.102788.

[16] D. Ponnaswami, O. Bilawar, S. Agasagi, R. Patil, and S. Maracharaddi, "Design and Analysis of Magnus Effect Mechanism on Wing for UAV Applications," *Tuijin Jishu/Journal Propuls. Technol.*, vol. 45, no. 03, pp. 1507–1513, 2024, doi: https://doi.org/10.52783/tjjpt.v45.i03.7437.

[17] Q. Zhang, "Application of magnus effect on wings," *Theor. Nat. Sci.*, vol. 9, pp. 180–186, 2023, doi: https://doi.org/10.54254/2753-8818/9/20240740.

[18] A. N. Alkhaledi, S. Sampath, and P. Pilidis, "Techno environmental assessment of Flettner rotor as assistance propulsion system for LH2 tanker ship fuelled by hydrogen," *Sustain. Energy Technol. Assessments*, vol. 55, p. 102935, 2023, doi: https://doi.org/10.1016/j.seta.2022.102935.

[19] N. R. Ammar and I. S. Seddiek, "Wind assisted propulsion system onboard ships: case study Flettner rotors," *Ships Offshore Struct.*, vol. 17, no. 7, pp. 1616–1627, Jul. 2022, doi: https://doi.org/10.1080/17445302.2021.1937797.

[20] J. Li, H. Lin, C. Sun, B. Jiao, G. Sun, and F. Cao, "Analysis of Aerodynamic Performance and Application of Flettner Rotor," *J. Inst. Eng. Ser. C*, vol. 105, no. 5, pp. 1373–1383, 2024, doi: https://doi.org/10.1007/s40032-024-01073-9.

[21] M. Reche-Vilanova, "Performance Prediction Program for Wind-Assisted Cargo Ships," 2020. doi: https://doi.org/10.13140/RG.2.2.24961.48480.